

We are IntechOpen, the world's leading publisher of Open Access books Built by scientists, for scientists

5,800

Open access books available

142,000

International authors and editors

180M

Downloads

Our authors are among the

154

Countries delivered to

TOP 1%

most cited scientists

12.2%

Contributors from top 500 universities



WEB OF SCIENCE™

Selection of our books indexed in the Book Citation Index
in Web of Science™ Core Collection (BKCI)

Interested in publishing with us?
Contact book.department@intechopen.com

Numbers displayed above are based on latest data collected.
For more information visit www.intechopen.com



Chapter

Use of Natural Safiot Clay for the Removal of Chemical Substances From Aqueous Solutions by Adsorption: A Combined Experimental and Theoretical Study

Aziz El Kassimi, Mohammadine El Haddad, Rachid Laamari, Mamoune El Himri, Youness Achour and Hicham Yazid

Abstract

The main objective of this work was to investigate the potential of Natural Safiot Clay (NSC), as an adsorbent for the removal of two cationic dyes such as Basic Blue 9 (BB9) and Basic Yellow 28 (BY28) from single and binary systems in aqueous solutions. For this, the effects of three factors controlling the adsorption process, such as initial dye concentration, adsorbent dose, and initial pH on the adsorption extent, were investigated and examined. The natural safiot clay was characterized using the following technique: energy-dispersive X-ray spectroscopy (EDX), scanning electron microscopy (SEM), DRX, and Fourier transform infrared (FT-IR) and pH of the point of zero charge (pH_{ZPC}). Energy-dispersive X-ray spectroscopy results indicate high percentages of Silica and Alumina. FT-IR spectrum identified kaolinite as the major mineral phase in the presence of quartz, calcite, and dolomite. The quantum theoretical study confirms the experimental results, through the study of the global and local reactivity and the electrophilicity power of the dyes. The electrophilicity power of dyes affects the removal efficiency. The theoretical study proves that BB9 ($\omega = 6.178$) is more electrophilic than BY28 ($\omega = 2.480$) and more interactions with surface sites. The results of the molecular dynamics simulation indicate that the dyes are adsorbed parallel to the surface of natural Safi clay (kaolinite), implying the strong interaction with the kaolinite atoms. All the results of quantum chemistry calculations and simulations of molecular dynamics are in perfect agreement with the results of the experimental study.

Keywords: adsorption, dyes; natural safiot clay, characterization, density functional theory

1. Introduction

The growth of humanity and the development of science and technology are causing an environmental disorder due to the pollution of water by a number of pollutants including synthetic dyes, which have a complex molecular structure, which makes them more stable and difficult. These dyes are discharged with the liquid effluents, which are most of the time directly discharged into watercourses without prior treatment [1]. These colored discharges pose a great threat to human health and the environment because many of the dyes are toxic. Therefore, it is very important to develop efficient methods for the removal of dyes from aqueous media.

Traditional processes such as biological processes give unsatisfactory results due to the composition of these releases of toxic and dyestuffs, which are difficult to biodegrade; on the other hand, physicochemical processes, which include coagulation-flocculation, oxidation, and membrane filtration, have been widely studied and have revealed a high efficiency in water discoloration [2, 3]. These techniques have proven to be very effective, but their high cost has prompted many researchers to try other cheaper and abundant materials. Adsorption, as a flexible, simple, and inexpensive approach, can be used for the removal of pollutant chemical species. Every day researchers describe new ways and elaborate a new adsorbent on the basis of good selectivity for a chemical species or for the low cost of the process. The elimination of dyes in aqueous solutions by adsorption on different solid materials, in particular on activated carbon, has been the subject of much work [4–6]. The adsorption of dyes on activated carbon has been found to be very effective, but its use remains limited due to the difficulties of its regeneration and its high cost [7].

For this reason, the use of clay as an adsorbent is of great interest because of its effectiveness, its accessible cost, and its abundance. From this perspective, lot of research has been done on clays and all have shown their depollution efficiency toward dyes [8, 9]. The importance given to these materials is granted to their abundant availability in nature and their great capacity of retention of various pollutants, which is offered by their structure in sheets, which gives a large specific surface toward the adsorption [10, 11].

In this context, our choice focused on clay, which is an adsorbent material found in abundance in Morocco, is effective and more economical. The use of clays for the depollution of waters contaminated by dyes requires a good knowledge of their mineralogical characteristics and of the mechanism of adsorption of these pollutants. On the other hand, Natural Safiot Clay (NSC) materials could be an attractive alternative for the adsorption of various pollutants from wastewater due to their low cost, their lamellar structure, which provides high specific surface areas, thermal stability, high cation exchange capacity, abundance, and high adsorption capacity [12–14].

Generally, most of the studies carried out to eliminate cationic dyes are carried out on single dyes [15], which lead us to study the possibility of eliminating a mixture of two dyes at the same time, close to the real conditions of effluents in the environment, because industrial discharges are a complex mixture of several pollutants.

Recently and with computer development, quantum chemistry calculations are widely used in studies of dye adsorption [16, 17]. A lot of research has been carried out on this theoretical approach; in particular since the appearance of their efficiencies in the study of adsorption mechanisms on the one hand, and the study of behavior of dyes with respect to the adsorbent surface on the other hand [18, 19]. The theoretical reactivity indices based on density functional theory (DFT) have become a powerful

and informative tool for studying organic reactivity and for describing intermolecular interactions [20, 21].

The purpose of this study was to demonstrate the ability of Natural Safiot Clay to remove some mixture industrial dyes such as Basic blue 9 and Basic yellow 28 from single and binary aqueous solutions. This allows optimizing the cost of the process and the quantity of the adsorbent used in the adsorption process to have a multiple removal efficiencies of different pollutants instead of one [22, 23]. In this study, the possibility of adsorption of Basic blue 9 (BB9) and Basic yellow 28 (BY28) in the single and binary system has been studied experimentally and theoretically using density functional theory (DFT) and molecular dynamics simulations (MDS), In order to explain the competitiveness between the two dyes on active sites and their reactivity, check if the experimental results are in good correlation with the theoretical results.

2. Materials and methods

2.1 Preparation of natural safiot clay

The Natural Safiot Clay (NSC) used in this work is collected from a natural basin in the region of Safi in Morocco for removal of Basic blue 9 and Basic yellow 28 from aqueous solutions and used without any prior activation. Samples were ground and sieved to obtain very fine particle sizes and washed with distilled water to ensure the removal of dust and any soluble impurities may exist.

2.2 Preparation of dyes solutions mixture

Basic blue 9 (BB9) and Basic yellow 28 (BY28) as representative cationic dyes were purchased from Sigma-Aldrich with a purity of 99% and used without further purification. The chemical structures of the studied dyes are given in **Figure 1**.

2.3 Experimentation conditions of adsorption studies

For single and binary system, several stock solutions 100 mg/L of BB9 and BY28 dyes have been prepared by mixing calculated volumes of the stock solutions of each dye and accurately diluting it with distilled water. The NSC and mixture of dyes are shaken in batch experiments at various parameters such as the amount of natural safiot clay (5 mg–35 mg), initial dye concentration (10 mg–40 mg/L), and initial solution pH (2–12). The working solutions' pH was adjusted to the desired values with dilute HCl (0.1 M) or NaOH (0.1 M) using a pH-Meter HANNA 5222. After stirring of a prescribed contact time, the solution is filtrated using filter syringe, and the maximum absorbance value of BB9 and BY28 is measured using spectrophotometer UV–Visible (JENWAY 6300) at 663 and 438 nm, respectively, as shown in **Figure 2**.

The percentage removal and the quantity adsorbed q_e (mg/g) of dye on NSC were calculated using the following equation:

$$\%Removal_{dye} = \frac{C_0 - C_e}{C_0} * 100 \quad (1)$$

$$q_e(mg/g) = \frac{C_0 - C_e}{m} * V \quad (2)$$

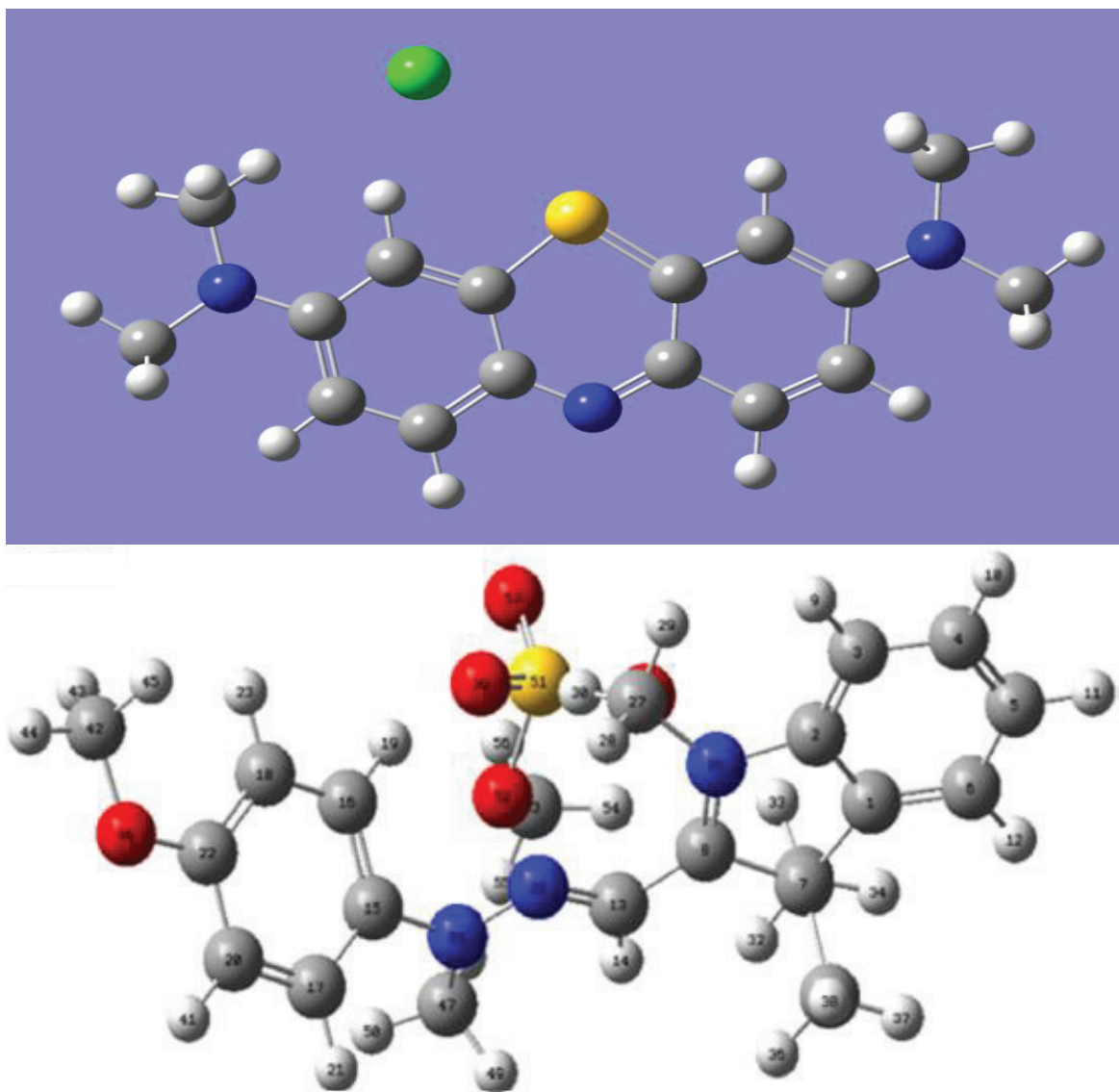


Figure 1.
Chemical structures of BB9 and BY28.

Where C_0 (mg/L) and C_e (mg/L) represent the concentration of BB9 and BY28 at initial and equilibrium, respectively, V (L) is the volume of solution, and W (g) is the weight of adsorbent used.

2.4 Surface characterization

The surface morphology, chemical composition, and the nature of functional groups responsible for adsorption of dyes onto the NSC adsorbent were studied by Scanning Electron Microscopy (SEM), Energy Dispersive X-ray spectroscopy (EDX), X-Ray Diffraction (XRD), and Fourier Transform Infrared (FT-IR).

2.5 Computational details

Density functional theory (DFT) is one of the most important tools of quantum chemistry of understanding popular qualitative chemical concepts such as energy of highest occupied molecular orbital (E_{HOMO}) and the lowest unoccupied molecular

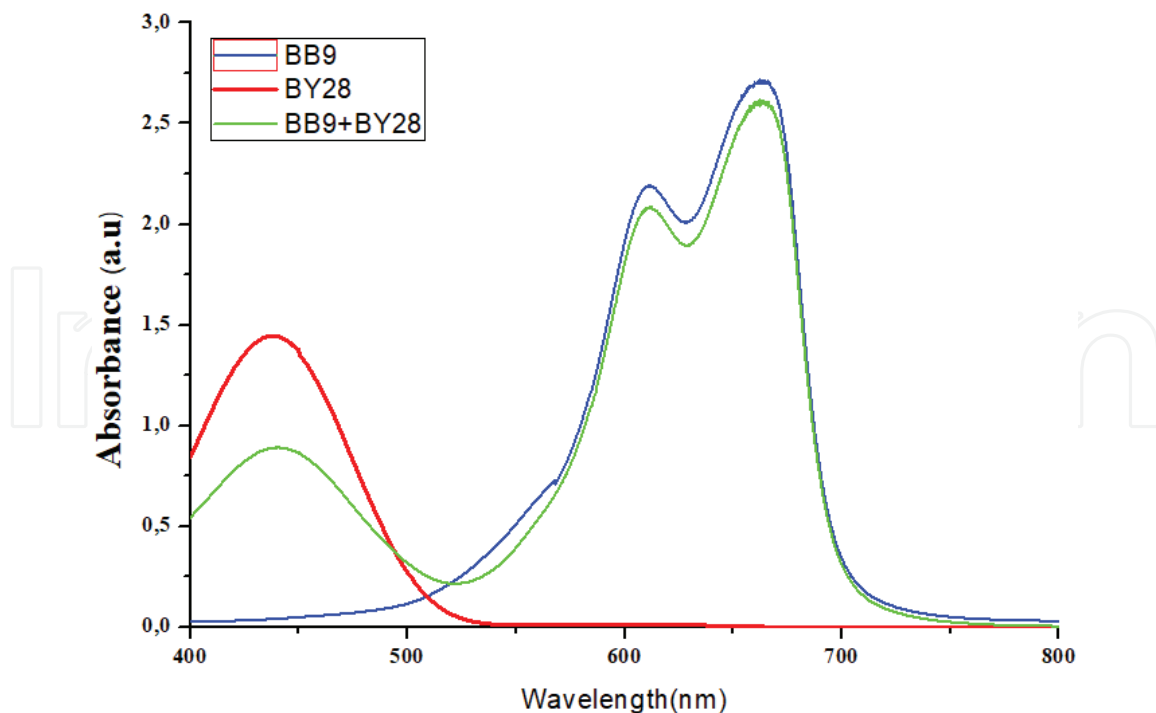


Figure 2.
 Absorption spectra of BB9, BY28, and their mixture.

orbital (E_{LUMO}), dipole potential (μ), hardness (η), softness (S), electrophilicity index (ω), and local reactivity descriptors such as Parr function $P(r)$ [24, 25]. All computations are carried out with the Gaussian 09 program. The geometries of dyes, BB9 and BY28, are optimized using density functional theory (DFT) at the B3LYP/6 G-31G (d) level. Optimizations are carried out using the Bery analytical gradient optimization method. The geometries optimized are characterized by positive vibrational frequency definite Hessian matrices [26].

When the values of E_{HOMO} and E_{LUMO} are known, one can determine through the following expressions [27] the values of the electronic chemical potential μ , the absolute hardness η , and the softness S as:

$$\mu = \frac{E_H + E_L}{2} \quad (3)$$

$$\eta = (E_L - E_H) \quad (4)$$

The global softness (S) introduced is the inverse of the global hardness [28]:

$$S = \frac{1}{\eta} \quad (5)$$

Using Parr's definition [29], the electrophilicity ω index is given by:

$$\omega = \frac{\mu^2}{2\eta} \quad (6)$$

Based on this idea, Domingo et al. [30] have introduced an empirical (relative) nucleophilicity index N , based on the HOMO energies obtained within the Kohn-Sham scheme and defined as:

$$N = E_{HOMO}(Nu) - E_{HOMO}(TCE.) \quad (7)$$

The HOMO energy of Tetracyanoethylene is -0.3351 a.u. at the same level of theory.

The electrophilic P_K^+ and nucleophilic P_K^- Parr functions, which allow for the characterization of the electrophilic and nucleophilic centers of a molecule, were obtained through the analysis of the Mulliken ASD (Atomic Spin Density) of the radical anion and the radical cation, respectively. These indices were obtained by single-point energy calculations over the optimized neutral geometries using the restricted B3LYP formalism for radical species. The results obtained will be compared with the experimental data.

The adsorption progress of the studied dyes on kaolinite surface is performed using Materials Studio (MS) 8.0 software developed by Accelrys Inc. The kaolinite crystal was optimized ($a = 5.196 \text{ \AA}$, $b = 9.007 \text{ \AA}$, $c = 7.372 \text{ \AA}$, and $\alpha = 93.029^\circ$, $\beta = 105.983^\circ$, $\gamma = 89.866^\circ$) and cleaved along the (001) plane, a vacuum slab with 10 \AA thickness was built. The final structure was enlarged to $(4 \times 2 \times 1)$ to provide a large surface for the interaction of the dyes [31].

3. Results and discussion

3.1 Characterization of natural safiot clay

3.1.1 Energy-dispersive X-ray spectroscopy

The spectrum of chemical constitution of natural safiot clay adsorbent is given in **Figure 3**. The EDX spectrum of **Figure 2** presents well-defined peaks, confirms the presence of the following chemical elements: Si, Al, Mg, Fe, K, P, S, O, Ca, C. These results confirm those found by the analysis XRF (**Table 1**), which also reveals the presence of these elements in the form of oxides: SiO_2 , Al_2O_3 , Fe_2O_3 , MgO , Na_2O , CaO , K_2O , TiO_2 . The atomic and mass percentages of the elements are summarized in **Table 2**. The predominance of silicon and oxygen peaks is clearly observed, which confirms the majority presence of kaolinite and quartz in the sample studied.

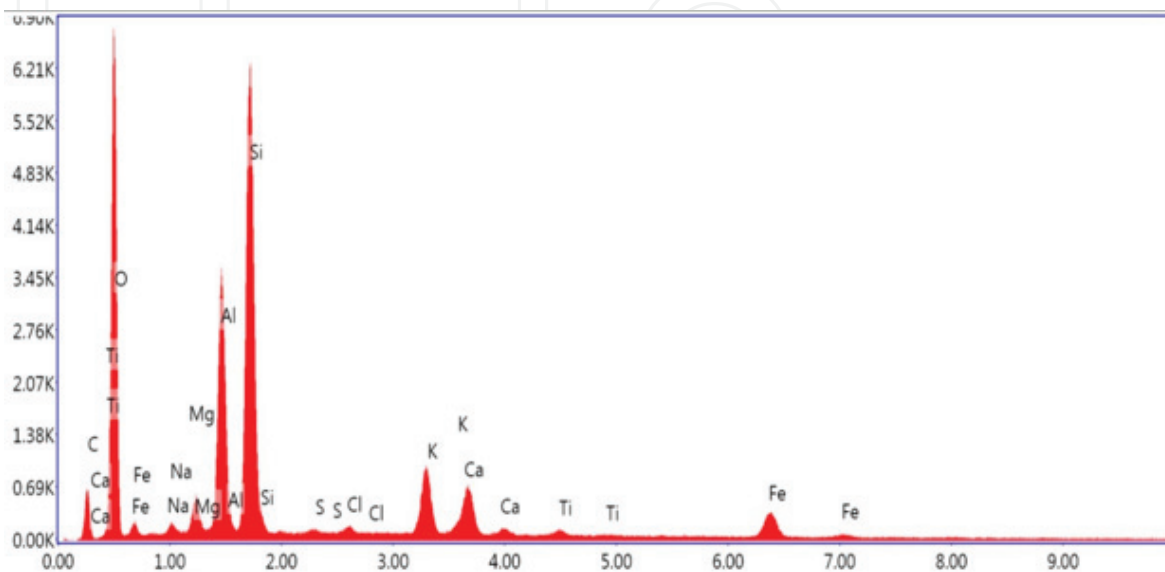


Figure 3.
EDX spectrum of natural safiot clay.

Dyes	Langmuir			Freundlich			Dubinin–Radushkevich			
	q _{max}	R _L	R ²	K _F	1/n	R ²	q _{max}	K _{D-R}	E	R ²
BB9 (S)	68.49	0.038	0.992	37.89	0.314	0.852	59.03	1 10 ⁻⁷	2236	0.925
BB9 (B)	41.15	0.015	0.996	25.71	0.222	0.566	44.78	1 10 ⁻⁷	2236	0.897
BY28 (S)	166.67	0.363	0.761	10.50	0.976	0.955	75.33	2 10 ⁻⁶	500	0.994
BY28 (B)	21.32	0.064	0.986	10.07	0.260	0.718	18.18	6 10 ⁻⁷	912.8	0.512

Table 1.
 Isotherm constants for BB 9 and BY28 in single and binary systems.

Eléments	% atomique	% massique
O	57.87	46.70
C	12.96	7.85
Na	0.59	0.68
Mg	1.25	1.53
Al	7.50	10.20
Si	13.78	19.52
K	2.18	4.30
Ca	1.70	3.43
Ti	0.19	0.47
Fe	1.72	4.85

Table 2.
 Atomic and mass percentage of the natural safiot clay constituents.

3.1.2 Fourier transform infrared spectroscopy

Fourier transform infrared (FTIR) analysis was applied to determine the functional groups present on the surface of natural safiot clay and understand its adsorption mechanism. FT-IR spectra of NS clay in the range of 400 cm⁻¹–4000 cm⁻¹ are taken to obtain information on the nature of functional groups at the surface of the adsorbent. The spectrum of natural safiot clay is shown in **Figure 4**. The band that stretches between 3200 and 3700 cm⁻¹ shows a peak with two shoulders at 3407 cm⁻¹ and 3610 cm⁻¹ corresponding to the vibrations of elongation of the hydroxyl group – OH linked to the water of constitution. In addition to the vibrations of deformation of the O-H bond due to the water molecules adsorbed between the sheets located at 1639 cm⁻¹. The bands that appear approximately around 3430 cm⁻¹ and 1630 cm⁻¹ correspond respectively to the vibrations of elongation and deformation of the OH group of the adsorbed water [32]. While the characteristic bands of carbonates are detected at 1436 cm⁻¹ and 2521 cm⁻¹ [33].

An intense absorption band at 900 cm⁻¹–1200 cm⁻¹ is centered on 1030 cm⁻¹, it characterizes the valence vibrations of the Si-O bond [34]. The bands between 795 and 748 cm⁻¹, coming from the Si-O-Al bond, also give way to a band around 778.4 cm⁻¹ [35]. The absorption band located at 1030 cm⁻¹ is in agreement with the X-ray

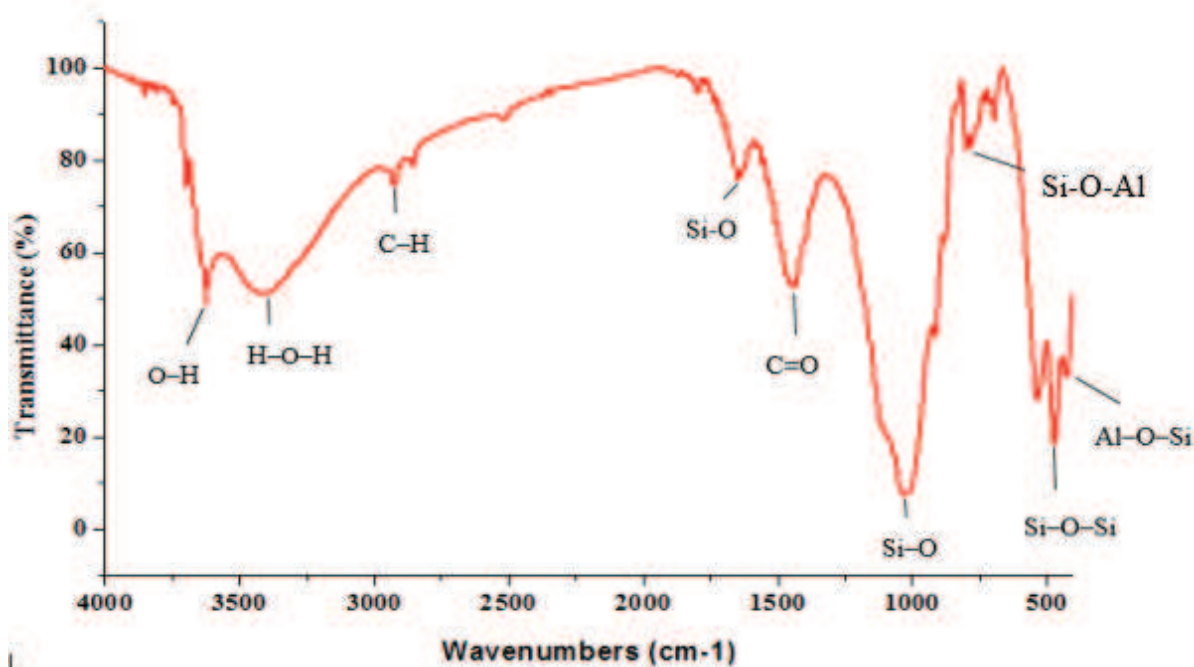


Figure 4.
FT-IR spectrum of natural safiot clay.

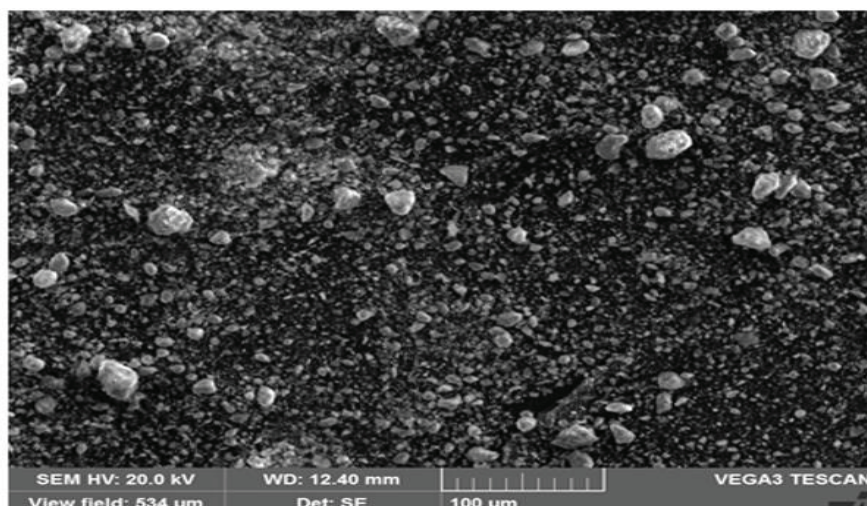
fluorescence indicating the presence of kaolinite in natural clay. However, the absorption bands at 423, 480, 534, 694, and 797 cm^{-1} correspond to quartz [36]. These results are in agreement with those found from XRF. They confirm the presence of quartz, carbonate, kaolinite, and dolomite in the clay studied.

3.1.3 Scanning electronic microscopy analysis

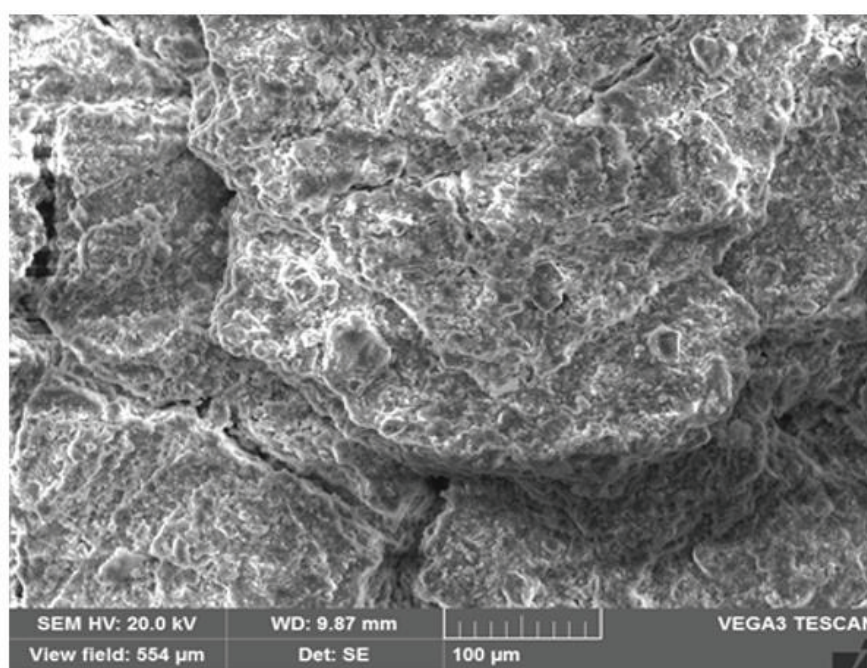
Scanning electronic microscopy (SEM) technique was carried out in order to observe the morphology, structure, and distribution of the grains of our adsorbent material studied. **Figure 5a** and **b** show the SEM micrographs of natural safiot clay before and after adsorption. The scanning electron microscope image (**Figure 5a**) shows aggregates of kaolin grains in spherical form and of heterogeneous size, the interstices between the grains form pores. We also observe large irregularly shaped cavities; this confirms the heterogeneous composition of our clay revealed by the XRD (kaolinite + calcite + vermiculite). In contrast, **Figure 5b** shows that the NSC surface is more homogeneous and saturated after adsorption.

3.1.4 XRD analysis

X-ray diffraction analysis allows us to identify the different mineralogical phases contained in our material. The X-ray diffraction patterns of NSC adsorbent are illustrated in **Figure 6**. This result demonstrated the principal presence of kaolinite characterized by an intense peak at $2\theta = 26.63^\circ$ ($2\theta = 26.63^\circ$; $d = 3.343 \text{ \AA}$) and a series of peaks with varying intensities at 12.33° , 19.75° , 40.85° and those of quartz at 20.87° , 37.92° , and 42.44° . In addition, the reflections spectrum at $2\theta = 8.62^\circ$, 29.47° , and 30.81° confirm the presence of illite, calcite, and dolomite, respectively. We see that the diagram also shows the presence of the peak corresponding to the following



(a)



(a)

Figure 5. SEM micrograph of the natural Safi clay before (a) and after (b) adsorption.

minerals: kaolinite, calcite, and vermiculite, which implies that our clay is heterogeneous.

3.1.5 Determination of pH zero-point charge

The pH zero-point charge (pH_{zpc}) plays an important role in the adsorption process. The point of zero charge (PZC) of our clay was determined using the pH drift method [37]. Six vials containing solutions of pH in the range of 2–12 (pH_i) and 50 mg of NSC are shaken for 24 h at room temperature, and the final pH was measured. The difference between the initial and final pH ($\Delta\text{pH} = \text{pH}_i - \text{pH}_f$) was plotted against the initial pH (pH_i) and the point where $\Delta\text{pH} = 0$ was taken as the point of zero charge. As shown in **Figure 7**, the pH_{zpc} of NSC was determined to be 7.2.

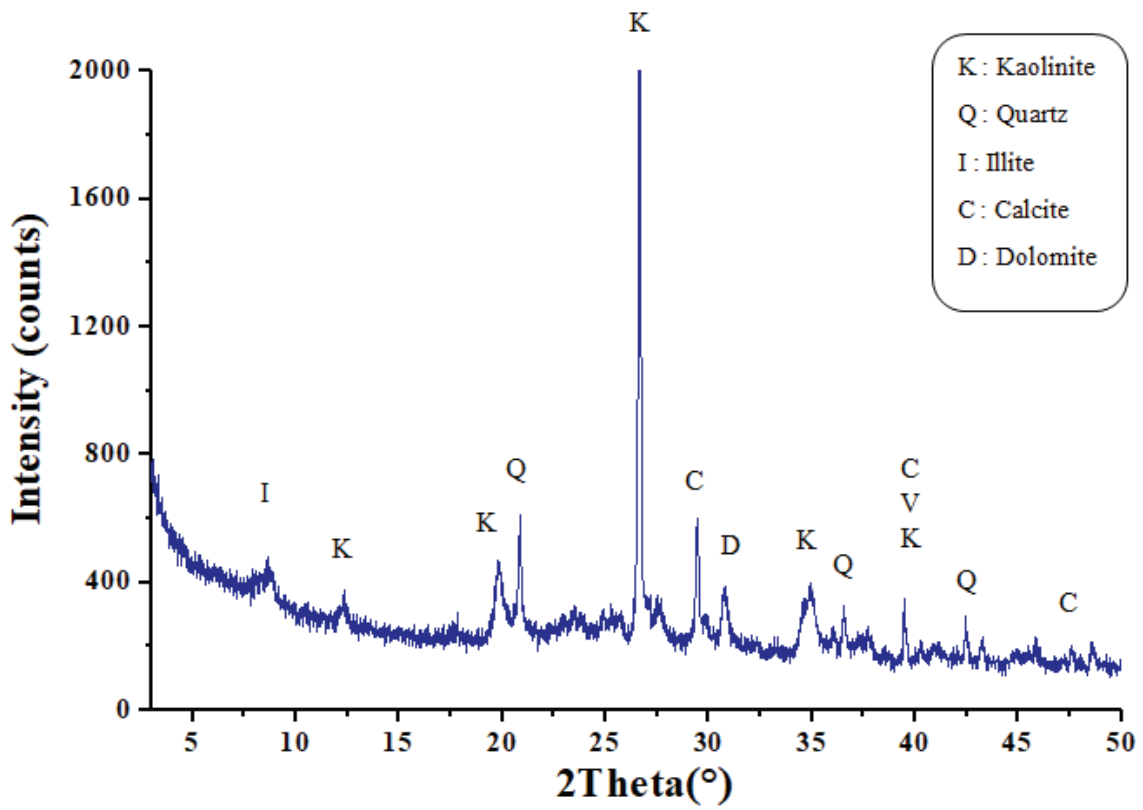


Figure 6. X-ray diffraction of natural safiot clay.

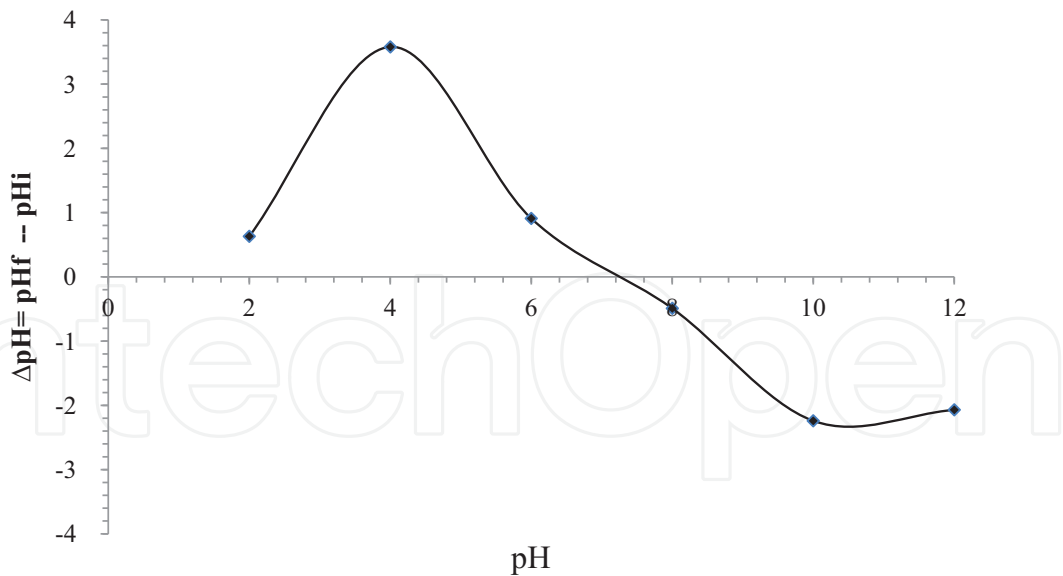


Figure 7. pHzpc values for natural safiot clay.

3.2 Experimental setup: single and binary adsorption studies

3.2.1 Effect of adsorbent dose

It is recognized that the effect of the adsorbent dose on the adsorption process is also considered to be one of the most important parameters that must be optimized,

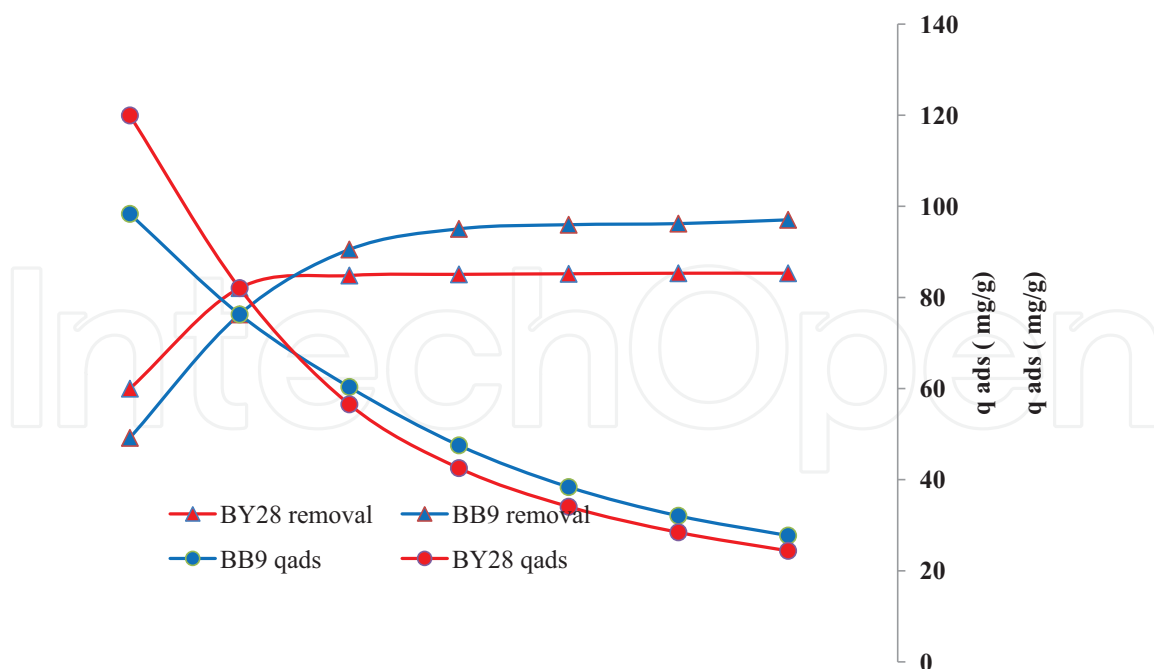


Figure 8. Effect of adsorbent amount on the removal efficiency and adsorption capacity of basic blue 9 and basic yellow 28.

since the mass of adsorbent has an effect on the adsorption capacity for a given initial concentration of the adsorbate under the operating conditions. The adsorption of BB9 and BY28 in single and mixture on natural safiot clay is studied by varying the mass of adsorbent from 5 to 35 mg in 50 mL solution of 20 mg/L dye concentration at a constant stirring rate of 60 minutes. From **Figure 8**, it can be observed that removal efficiency of the dye increases from 49.17% to 97.03% for BB9 and from 59.97% to 85.32% for BY28 as adsorbent dose is an increase from 5 to 35 mg. This is because of the extra number of adsorption sites accessible with an increase in the adsorbent dose. On the other hand, the dye uptake capacity reduces from 98.34 to 27.72 mg/g and from 119.9 to 24.38 mg/g for BB9 and BY28, respectively. This can be attributed to the unsaturation of adsorption sites through the adsorption reaction with increasing adsorbent dosage [38, 39]. Another important reason is that at high adsorbent dosage, the available dye molecules are deficient to completely cover the available binding sites on the natural safiot clay, which results in low solute uptake [40, 41]. Similar results have been reported previously by other researchers for the adsorption of dyes by different material [42–44]. The optimum adsorbent dose is fixed conveniently at 30 mg per 50 mL of solution dye for the following studies.

3.2.2 Effect of initial dye concentration

The effect of initial concentrations of BB9 and BY28 dyes is examined at different initial concentrations ranging from 10 to 40 mg/L on the adsorption capacity and removal efficiency onto natural safiot clay. As seen from **Figure 9**, the adsorption capacity increases from 22.58 to 58.45 mg/g for BB9 and of 12.68 to 58.89 mg/g for BY28. In this case, the % removal decreases from 98.97% to 87.67% and from 87.67% to 70.08% for BB9 and BY28, respectively. These results indicate that the adsorption sites of NSC adsorbent for dyes adsorption are still unsaturated

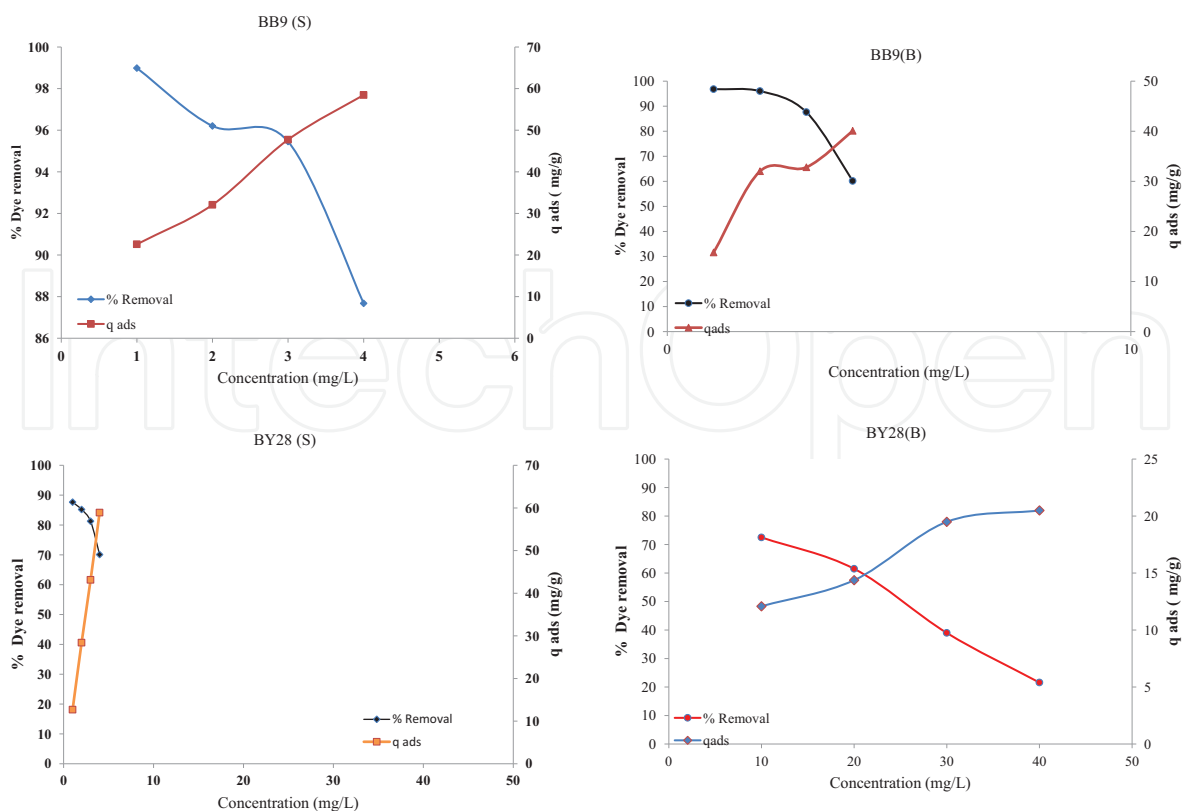


Figure 9.

Effect of the initial dye concentration on the adsorption capacity and removal efficiency of BB9 and BY28, in single (S) and binary (B) system onto NSC.

within the dye concentration range. In addition, increasing initial dyes' concentrations increases the number of collisions between dyes ions and the surface area of NSC adsorbent, which enhances the adsorption process [45]. Similar results had been reported by Auta and Hameed [46] for MB dye removal onto modified ball clay chitosan composite.

3.2.3 Effect of initial dye pH

The initial pH of the aqueous solution is important parameter controlling the adsorption process, where it affects both the degree of ionization of the dye and the surface properties of the adsorbent. The effect of initial pH of dye solution on the percentage removal of dye is studied by varying the initial pH from 2 to 12 under constant process parameters onto NSC, and results are presented in **Figure 10**. It is revealed that pH has practically a small effect on the percentage removal of the two basic dyes in simple system. In binary system, BY28 percentage removal is increased from 34.74% to 71.14% when pH is varied from 2 to 12 and also for BB9 percentage removal increase from 90.86% to 96.75%. These results are explained by pH zero-point charge pH_{ZPC} , the pH_{zpc} of any adsorbent is a very important characteristic that determines the pH at which the surface has net electrical neutrality. In explaining this behavior by the fact that the negative charge dominates the adsorbent's surface in the basic medium. Thus, an electrostatic attraction exists between the negative charges of OH deposited on the clay surface and the positive charges of the dyes. Moreover, an electrostatic attraction between BB9 and BY28 dyes and the positive charge on the surface of NSC at low pH are evident [47, 48].

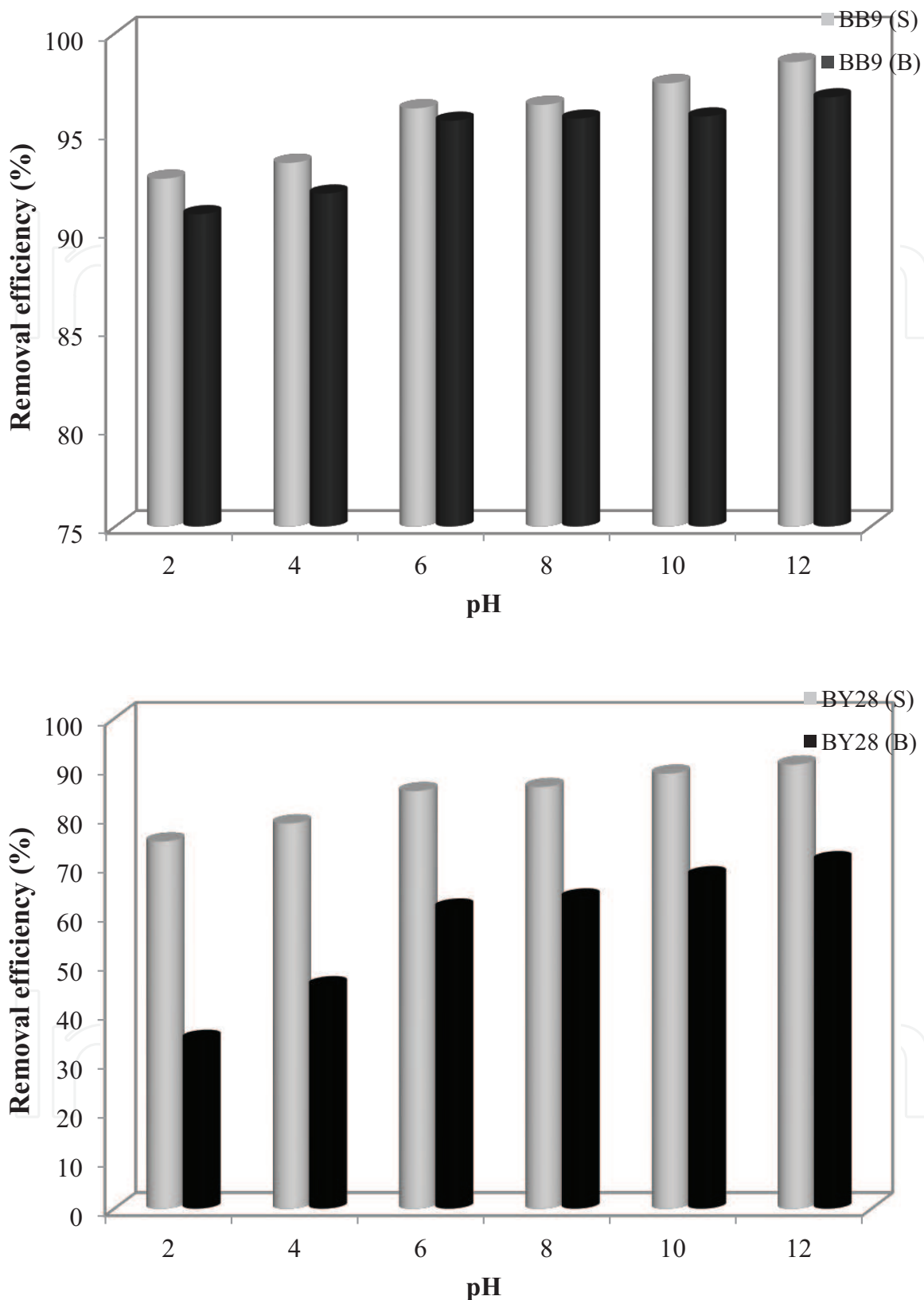
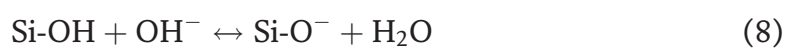
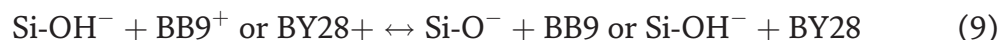


Figure 10.
 Effect of initial dye pH on the removal efficiency (%) of BB9 and BY28 dyes in single and binary solutions.

Consequently, the mechanism proposed can be described by the following equation.





Similarly, the montmorillonite, bentonite clay, and montmorillonite/CoFe₂O₄ composite adsorption capacities were studied as a function of pH, and it was observed that maximum basic blue 9 dye adsorption was in acidic pH range [49–51].

3.2.4 Competitive adsorption between BB9 and BY28

BB9 and BY28 adsorption in single and binary adsorption systems onto NSC is studied and is illustrated in **Figure 11**. The removal efficiency decreased in binary systems (as compared with single dye systems), the reduction was from 96.20% to 95.57% and from 85.32% to 61.48% for BB9 and BY28, respectively. For these results it is clear in the binary system, BB9 dye is most dominant and BY28 is most recessive dye. The values of R% also show that adsorption of BB9 and BY28 is reduced by the presence of other dyes in solutions within reduction percentage of 0.66% and 27.94% for BB9 and BY28, respectively. This behavior can be explained by the competitive adsorption between BB9 and BY28 for active sites with that BB9 dye is the first to be adsorbed in the active sites and by that BB9 is more electrophilic than BY28. This result will be demonstrated by following quantum chemicals study.

3.3 Adsorption isotherms

Adsorption isotherms play an important role in the determination of the maximum adsorption capacity and the identification of the type of adsorption. The results of the adsorption experiments were analyzed per the well-known models of Langmuir, Freundlich, and Dubinin–Radushkevich (D-R):

The Langmuir isotherm is valid for monolayer adsorption on surface containing a finite number of identical sites [52]. The linear form of the Langmuir isotherm can be represented by the following equation:

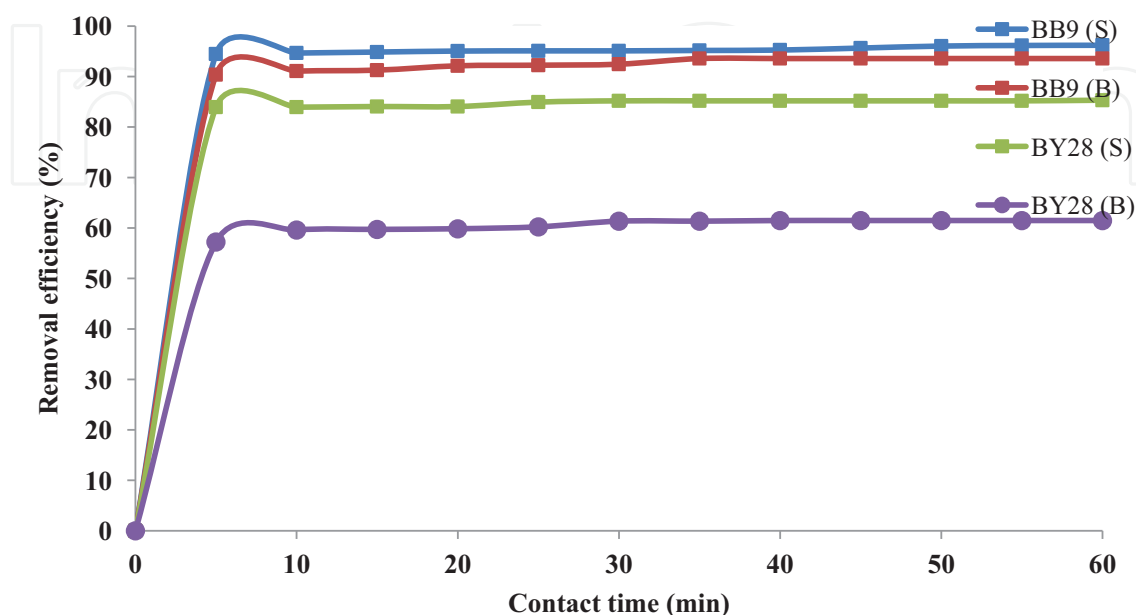


Figure 11. Adsorption competition of BB9 and BY28 onto NSC adsorbent sites.

$$\frac{C_e}{q_e} = \frac{1}{q_m K_L} + \frac{1}{q_m} C_e \quad (10)$$

Where C_e (mg/L) represents the equilibrium concentration of the adsorbate, q_e the amount adsorbed at equilibrium (mg/g), K_L (L/mg) and q_m (mg/g) are the Langmuir constant and the maximum amount of adsorbate, respectively.

To confirm the favorability of the adsorption process, the separation factor R_L was calculated by the following Equation [53]:

$$R_L = \frac{1}{1 + K_L C_0} \quad (11)$$

where the adsorption process is unfavorable ($R_L > 1$), linear ($R_L = 1$), favorable ($0 < R_L < 1$), or irreversible ($R_L = 0$). Here, R_L values for the adsorption of dyes are less than 1 and greater than 0, indicating favorable adsorption.

Freundlich isotherm model is an empirical equation based on sorption on a heterogeneous surface or surface supporting sites of varied affinities [54]. The linearized Freundlich model is represented by the following equation:

$$\log(q_e) = \log(K_f) + \frac{1}{n} \log(C_e) \quad (12)$$

where K_f (mg/g) is the measurement of adsorption capacity, and $1/n$ is the adsorption intensity of the adsorbent.

The Dubinin–Radushkevich model is a more generalized model as compared with the Langmuir isotherm and often used to estimate the characteristic porosity and the apparent free energy of adsorption [55]. The linearized Dubinin–Radushkevich (D-R) isotherm model is represented by the following equation:

$$\ln(q_e) = \ln(q_m) - B\epsilon^2 \quad (13)$$

where q_m is the theoretical saturation capacity (mg/g), B is the D-R constant related to the sorption energy (mol^2/kJ^2), and ϵ represents the Polanyi potential (J/mol), which is determined by:

$$\epsilon = RT \ln \left(1 + \frac{1}{C_e} \right) \quad (14)$$

R is the universal gas constant ($8.314 \text{ J mol}^{-1} \text{ K}^{-1}$), and T is the absolute temperature (K). The mean free energy of adsorption E calculated from B using the following relation:

$$E = \frac{1}{\sqrt{2B}} \quad (15)$$

The main parameters, characterizing each model as well as the coefficients of determination (R^2), are grouped in **Table 1**. Comparison with Freundlich and Dubinin–Radushkevich model shows the high correlation coefficient of Langmuir isotherm for both dyes in single and mixture systems. This result suggests that the dye was homogeneously adsorbed on a monolayer surface of the adsorbent.

The value of parameter $1/n$ of the Freundlich equation gives an indication of the validity of the adsorption of the adsorbent adsorbate system. The values of $1/n$ presented in **Table 1** are between 0 and 1 indicating that the adsorption of the two dyes on our prepared adsorbent material (NSC) is favorable.

The magnitude of E is useful for estimating the type of adsorption process. The found values of E for BB9 and BY28 in the single and binary system are less than 8 kJ mol^{-1} , knowing that energy values less than 8 kJ mol^{-1} indicate physisorption and energy values varying from 8 to 16 kJ mol^{-1} indicate chemisorption. Therefore, the adsorption type of BB9 and BY28 onto NSC has been defined as physical adsorption (physisorption). This confirms the results following the study of the influence of pH.

3.4 Kinetics of adsorption

The kinetic of adsorption is an important characteristic in evaluating the efficiency of adsorption process. Three kinetics models (pseudo-first order, pseudo-second order, and intraparticle diffusion) were utilized to test the experimental data and predict the controlling mechanism of dye adsorption process.

3.4.1 Pseudo-first-order model

The linearized form of pseudo-first-order rate expression is given as:

$$\log(q_e - q_t) = \log(q_e) - \frac{k_1}{2.303}t \quad (16)$$

Where q_e and q_t are the amount of dye adsorbed on sorbent (mg/g) at equilibrium and time t , respectively, k_1 corresponds to the reaction rate constant of pseudo-first-order (min^{-1}), and t is time (min) [56]. The values of q_e and k_1 were calculated from the slope and intercept of the plots of the $\log(q_e - q_t)$ vs. t .

3.4.2 Pseudo-second-order model

Pseudo-second-order rate expression reaction model is expressed as (linearized form) [57]:

$$\frac{t}{q_t} = \frac{1}{k_2 q_e^2} + \frac{1}{q_e}t \quad (17)$$

Where k_2 is the pseudo-second-order rate constant ($\text{g/mg}\cdot\text{min}$). A plot of t/q_t and t should give a linear relationship if the biosorption follows pseudo-second-order model. The q_e and k_2 can be calculated from the slope and intercept of the plot.

3.4.3 Intraparticle diffusion model

The intraparticle diffusion model is based on the theory proposed by Weber and Morris [58]. The Weber and Morris equation is (18):

$$q_t = k_{id}t^{1/2} + C \quad (18)$$

Dyes concentration (mg/l)		Pseudo-first order				Pseudo-second order			Intraparticle diffusion		
		qe,exp	qe,cal	K ₁	R ²	qe,cal	K ₂	R ²	Ki	C	R ²
BB9 (S)	10	15.48	7.998	0.028	0.752	15.78	0.198	0.999	0.095	16.20	0.965
	20	32.07	0.857	0.037	0.668	31.34	0.156	1.000	0.114	30.24	0.976
	30	47.72	1.795	0.074	0.403	47.85	0.109	1.000	0.306	45.66	0.794
	40	58.45	8.707	0.061	0.783	58.82	0.022	0.999	0.927	51.51	0.971
BY28(S)	10	12.69	0.129	0,112	0,485	12.73	0,470	1.000	0,100	12.04	0,542
	20	28.39	0.823	0,070	0,826	28.49	0,246	1.000	0,098	27.72	0,798
	30	43.14	2.960	0,023	0,913	42.37	0,071	0,999	0,316	39.86	0,905
	40	58.89	96.11	0,285	0,858	59.88	0,020	0,999	1.499	49,17	0,825
BB9(B)	10	15.80	23.22	0.041	0.484	15.82	1.051	1.000	0.036	15.54	0.756
	20	32.01	1.376	0.054	0.892	32.05	0.191	1.000	0.217	30.45	0.843
	30	43.82	8.586	0.064	0.937	44.05	0.031	0.999	0.881	37.27	0.982
	40	48.00	51.54	0.059	0.812	50.76	0.003	0.960	4.923	9.712	0.954
BY28(B)	10	12.08	3.088	0.177	0.813	12.16	0.209	0.999	0.131	11.19	0.873
	20	14.37	12.58	0.217	0.851	14.45	0.200	0.999	0.112	13.58	0.879
	30	19.49	12.36	0.165	0.898	19.68	0.087	0.999	0.423	16.69	0.649
	40	20.49	1.173	0.170	0.756	20.57	0.332	1.000	0.167	19.42	0.502

Table 3. Kinetics parameters for the adsorptive removal onto NSC adsorbent of BB9 and BY28 dyes and their mixture.

Where q_t is the adsorption capacity (mg/g) at time t (min), k_{id} is the intraparticle diffusion rate constant (mg/g.min), and C (mg/g) is a constant, which provides the information regarding the thickness of the boundary layer. The values of K_{id} and C were calculated from the slope and intercept of the plots of the q_t against $t^{1/2}$.

The conformity between the experimental data and the predicted model is based on the values of the correlation coefficients (R^2), hence the value R^2 closest to unity will indicate the adequate model to correctly describe the kinetics of adsorption of the dye.

Table 3 summarizes the rate constants and correlation coefficients (R^2) of the three kinetic models. The fitting of the kinetic data in the pseudo-second-order equation showed excellent linearity with high correlation coefficient ($R^2 > 0.999$), and the good agreement between the experimental and calculated equilibrium adsorption for the pseudo-second-order model confirms that this one describes correctly the adsorption kinetics. Similar results have been observed in the adsorption of basic dyes onto Moroccan Clay [59] and in the adsorption of Methylene Blue (MB) by montmorillonite clay [60].

3.5 Quantum chemical studies

3.5.1 Global reactivity descriptors

The global chemical reactivity descriptors, energy gap (ΔE), dipole moment (μ), hardness (η), softness (S), nucleophilicity (N), and electrophilicity index (ω) with

Dyes	BB9	BY28
E_T (u.a)	-1643.18	-1754.96
μ (Debye)	11.351	7.573
E_{HOMO} (eV)	-4.373	-5.585
E_{LUMO} (eV)	-3.210	-2.387
μ (eV)	-3.791	-3.986
η (eV)	1.163	3.198
S (eV)	0.859	0.312
ω (eV)	6.178	2.480
N (eV)	4.747	3.535

Table 4.
Quantum chemical parameters of the studied dyes calculated at B3LYP/6 G-31G (d).

calculated from HOMO and LUMO energies and are obtained at the level of theory B3LYP/6 G-31G(d) and summarized in **Table 4**.

Energy gap ($\Delta E_{gap} = E_{HOMO} - E_{LUMO}$): The energy gap between the HOMO and LUMO is very important in determining the chemical reactivity of the molecule dyes toward the adsorption on the adsorbent surface. On the other hand, the decrease in the value of ΔE_{gap} increases the reactivity of the molecule, which facilitates adsorption and increases the adsorption efficiency. It can be seen from **Figure 12** that the BB9 dye shows a lower ΔE_{gap} ($\Delta E_{gap} = 1.163$ eV) compared with the BY28 dye, which has a difference of 3.198 eV, which clearly means that the molecule of BB9 is more reactive than BY28, Therefore, the BB9 dye will be adsorbed firstly. This conclusion is in agreement with the experimental results.

Dipole moment (μ): The dipole moment (μ) is another important electronic parameter, provides information on the polarity of the whole molecule. The high

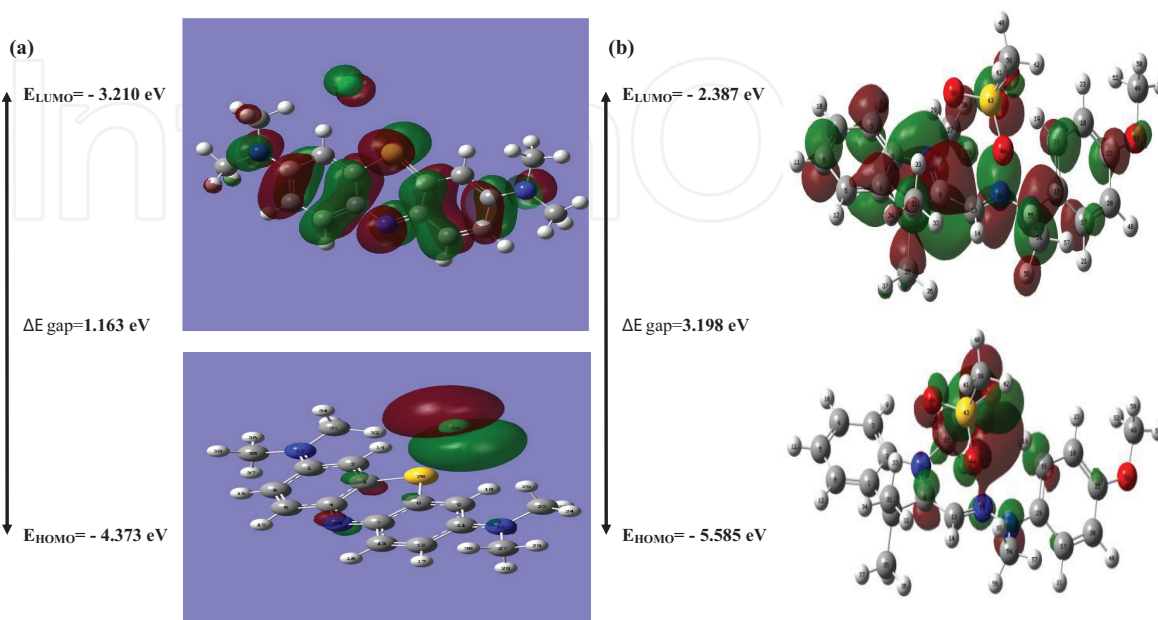


Figure 12.
Highest occupied molecular orbital (HOMO) and the lowest unoccupied molecular orbital (LUMO) density of BB9 (a) and BY28 (b) BY DFT at the B3LYP/6 G-31G(d).

molecular polarity probably gives rise to great chemical reactivity. It is clearly established in the literature that molecules with high dipole moments are more reactive, and their action results in a significant elimination efficiency. In our case the high dipole moment value of BB9 (11.351 D) probably increases the adsorption between the BB9 dye and the surface of natural clay compared with BY28 (7.573 D), which explains the adsorption efficiency higher than BB9 when compared with BY28 and confirms the experimental results.

Hardness (η) and softness (S): The stability and reactivity of a molecule are determined by the calculation of two important parameters: the global hardness (η) and the softness (S). The resistance of a molecule to deformation is determined by the chemical hardness, a hard molecule has a high energy gap. In addition, a soft molecule has a low energy gap. It is important to note that electronic systems with hard molecules have the least tendency to react while systems with soft molecules have a higher tendency to react.

The high percentage of elimination of a molecule is linked to a low value for chemical hardness and a high value for softness. In the present work, the values of the global hardness (η) and the softness (σ) presented in **Table 5** clearly show that the BB9 dye has the lowest value of the hardness ($\eta = 1.163$ eV) and the higher value of the softness ($S = 0.859$ eV), which explains their significant elimination percentage compared with BY28, these results are in good agreement with the experimental results.

Global electrophilicity index (ω): The global electrophilicity index (ω) represents the capacity of the dyes to accept electrons. More reactive nucleophilic is characterized by lower value of ω , and conversely more reactive electrophilic is characterized by a higher value of ω . From **Table 5**, we notice that the electrophilicity value of BB9 ($\omega = 6.178$) is greater than that of BY28 ($\omega = 2.48$); this indicates that the molecule of BB9 is more electrophilic than that of BY28. Consequently, BB9 will be adsorbed first followed by BY28.

Dye	N° of atoms	Atoms	P_k^+	P_k^-	ω_k	N_k
BB9	1	C	0.117052	-0.091655	0.72314726	—
	2	C	-0.083178	0.109989	—	0.52134786
	3	C	0.123453	-0.0193705	0.76269263	0.09195176
	4	C	-0.0825946	0.0874818	-0.51026944	0.4152761
	5	C	0.1346605	-0.0391588	0.83193257	0.18588682
	6	C	-0.044701	0.0617533	-0.27616278	0.29314292
	7	C	-0.0622537	0.0077143	-0.38459903	0.03661978
	8	C	0.1288878	-0.049104	0.79626883	0.23309669
	9	C	-0.0873976	0.0988698	-0.53994237	0.46933494
	11	C	0.1294818	-0.031639	0.79993856	0.15019033
	12	C	-0.045136	0.063713	—	0.30199962
	13	C	0.1402246	-0.0370003	0.86630758	0.17564042
	19	N	0.3640112	-0.0556138	2.24885996	—
	20	S	0.1232636	-0.0137067	0.76152252	—
	21	N	0.0351644	0.09916571	0.21724566	0.47073963
	22	N	0.0643843	0.15539811	0.39776621	0.73767483

Dye	N° of atoms	Atoms	P_k^+	P_k^-	ω_k	N_k
	23	C	-0.0038013	-0.006641	—	—
	27	C	-0.0035767	-0.00689	—	—
	31	C	-0.0061814	-0.005169	—	—
	35	C	-0.0061321	-0.010607	—	—
	39	Cl	0.0012179	0.5782508	0.00752419	2.74495655
BY28	1	C	0.040255	0.066561	0.105689697	0.23709028
	2	C	-0.000773	0.00887	—	0.03159494
	3	C	0.045305	0.037015	0.118214337	0.13184743
	4	C	-0.025946	-0.014818	—	—
	5	C	0.066052	0.091588	0.172349484	0.32623646
	6	C	-0.021701	-0.037533	—	—
	7	C	-0.036225	0.001143	—	0.00407137
	8	C	0.458878	-0.089904	1.197350365	—
	13	C	-0.173976	0.168698	—	0.60090228
	15	C	-0.014488	0.091639	—	0.32641812
	16	C	0.022465	0.020003	0.058617925	0.07125069
	17	C	0.03011	-0.006138	0.078566023	—
	18	C	-0.011644	0.016571	—	0.05902590
	20	C	-0.013843	0.039811	—	0.14180678
	22	C	0.026365	0.07067	0.068794195	0.25172654
	24	N	0.121797	0.125083	0.317804912	0.44554565
	25	N	0.362411	-0.068898	0.945639022	—
	26	N	0.059207	0.13669	0.154488825	0.48688978
	27	C	-0.006573	-0.003929	—	—
	31	C	0.019834	0.001078	0.051752856	0.00383984
	35	C	0.016503	0.000443	0.043061278	0.00157797
	39	O	0.000958	0.10219	0.002499709	0.36400078
	40	O	0.00195	0.081069	0.005088135	0.28876778
	42	C	-0.000314	-0.005534	—	—

Table 5.
Theoretical prediction of reactive sites using Parr function for BB9 and BY28 dyes.

3.5.2 Local molecular reactivity

The local reactivity site of the studied dyes has been analyzed by evaluating Parr functions (PF). The PF is used to obtain the detail information of local reactivity of each atom in the molecule. Domingo proposed the Parr functions $P(r)$ [61], which are given by the following equations:

$$P^{+(r)=\rho_s^{\text{ra}}(r)} \quad \text{for nucleophilic attack} \quad (19)$$

$$P^-(r) = \rho_s^{\text{rc}}(r) \quad \text{for electrophilic attack} \quad (20)$$

With these electrophilic and nucleophilic Parr functions are at hand, the local electrophilicity ω_K and the local nucleophilicity N_K indices will be redefined as follows:

$$\omega_K = \omega P_K^+ \quad (21)$$

$$N_K = N P_K^- \quad (22)$$

Table 5 shows that at the DFT level, the most susceptible site to a nucleophilic attack for BB9 is located on sulfur, nitrogen, and benzene ring. In the case of an electrophilic attack, the most reactive site is on Cl39. For BY28 the more susceptible sites to nucleophilic attacks are nitrogen and C8 atoms, while N26 and C13 are the most susceptible sites for electrophilic. The results indicated that the BB9 dye has more and strong electrophilic sites than BY28; consequently, BB9 has a high affinity for NSC than BY28.

3.5.3 MC and MD simulations

In this study, Monte Carlo simulations were performed to study the adsorption and orientation of dyes on charged surfaces based on (001) kaolinite surface and all-atom models. The most stable low-energy adsorption configurations of the studied dyes are shown in **Figure 13**. It is clear that the three dyes examined BB9, BB41, and BY28 are adsorbed almost parallel to the plane to maximize surface and contact coverage. These adsorption configurations indicate that there are strong interactions between the studied dyes and the kaolinite atoms. This facilitates their adsorption to the surface of the kaolinite (001) by blocking a maximum of sites and ensuring a great influence on the removal efficiency.

The outputs and descriptors calculated by the Monte Carlo simulation are presented in **Table 6**. The parameters presented in **Table 6** include total energy, in kcal mol⁻¹, of the substrate-adsorbate configuration. As can be seen from **Table 6**, BB9 gives the maximum adsorption energy in negative value found during the simulation process. High values of adsorption energy indicate that BB9 molecule will give the highest removal efficiency and strong interaction between a kaolinite substrate and the studied dye. These results are in good agreement with experimental findings.

To further confirm our results, we have performed the energy fluctuation curves as obtained from MD simulations; the equilibration of the system is confirmed by the stable mean values of energy fluctuations, as shown in **Table 7**. The mean square displacement (MSD) and the diffusion coefficient were calculated after 100,000 steps. The obtained data included in **Table 7** show that the diffusion coefficient of the free water molecules was more pronounced (5.85×10^{-6} cm²/s) than the water with BB9 and BY28 molecules. Much smaller diffusion coefficients obtained for water with BB9 were caused by the strong interaction between (water + BB9) and the kaolinite surface, which decreased the mobility of the water [62].

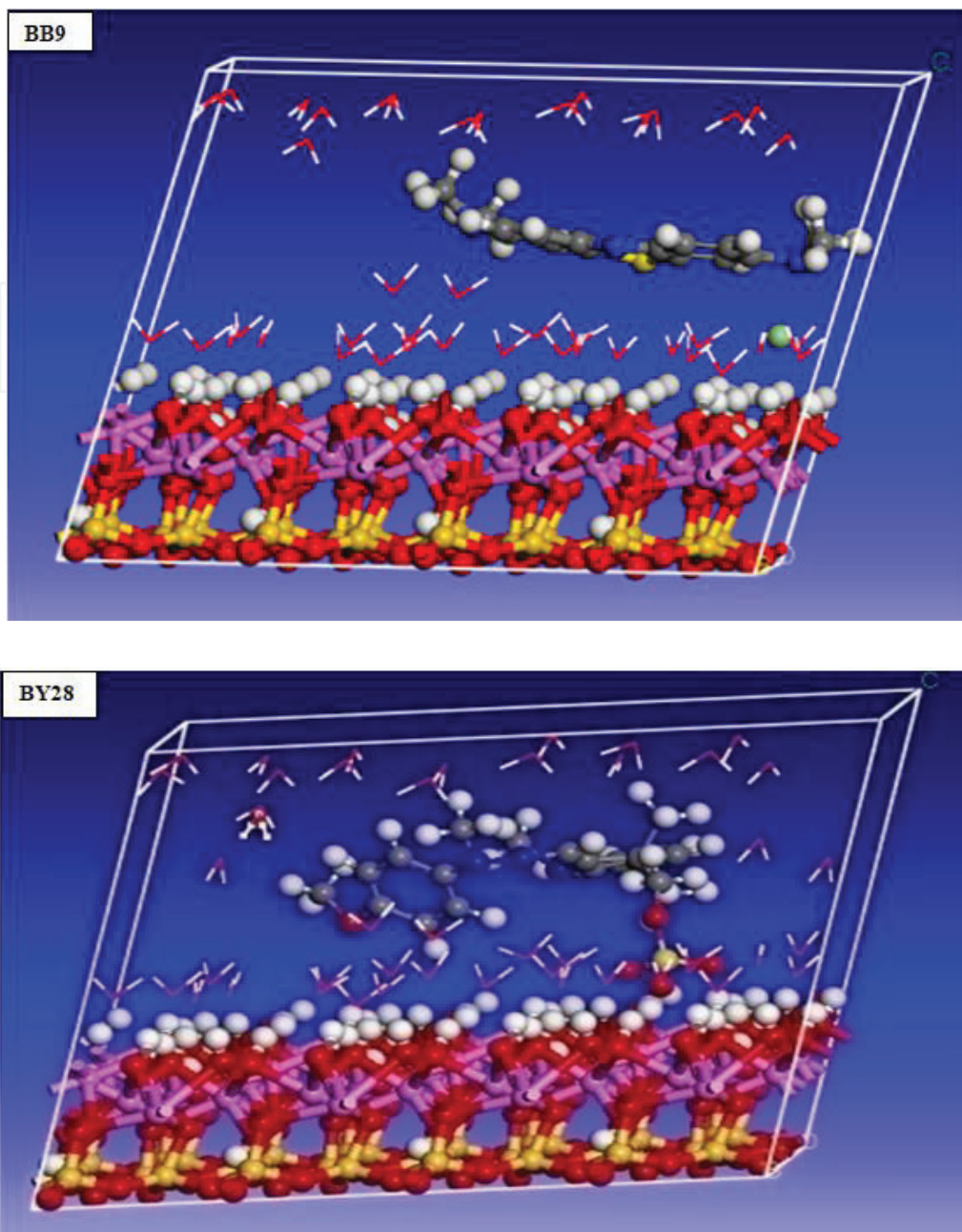


Figure 13. The most stable low-energy configuration for the adsorption of the dyes on kaolinite surface obtained through the Monte Carlo simulations.

System	Total energy	Adsorption Energy	Rigid adsorption energy	Deformation energy	Ead/Ni Dye
BB9/(001)	-111.4	-317.53	-150.77	-166.5	-317.53
BY28/(001)	-213.8	-146.92	-117.07	-29.89	-147.18

Table 6. Outputs and descriptors calculated by the Monte Carlo simulations for the lowest adsorption configurations of tested dyes on kaolinite (001) surface (in kcal/Mol).

Conditions	Diffusion coefficient of water ($10^{-6} \text{ cm}^2/\text{s}$)
Free water molecules	5.850
Water with BY28	2.430
Water with BB9	0.450

Table 7.
Calculated diffusion coefficient of free water and water with dyes in kaolinite surface.

4. Conclusion

The results obtained in this research indicated that natural safiot clay was considered low cost, eco-friendly, and a promising alternative adsorbent for removing BB9 and BY28 dyes in single and binary systems from an aqueous solution. The percentage of dye removed increased with increasing adsorbent dosage, decreased with increasing initial dye concentration, and varied with dye solution pH. The rate of adsorption was found to obey pseudo-second-order kinetics model with a good correlation coefficient indicating toward chemisorption, and the Langmuir isotherm represented the equilibrium adsorption and shows monolayer homogeneous surface of adsorbent for single and binary mixture.


All the theoretical parameters of DFT calculations show that the two dyes can be adsorbed and that the BB9 molecule has the best percentage of elimination. From this calculation, we note that: The dye removal efficiency increases with the highest values of ω , E_{LUMO} , μ , and S and the lowest values of ΔE_{gap} , E_{HOMO} and η . Another important conclusion that we can draw from these calculations is that the theoretical results from reactivity descriptors show that nitrogen, sulfur, carbon, and nitrogen atoms of BB9 and BY28 are the main adsorption sites, respectively. Finally, this study displays a good correlation between the theoretical and experimental data, which confirm the reliability of the quantum chemical methods to study the competitive adsorption of two cationic dyes onto NSC surfaces, in the single and binary system. DFT calculations, Monte Carlo method, and Molecular dynamics simulations support the experimental findings.

Author details

Aziz El Kassimi*, Mohammadine El Haddad, Rachid Laamari, Mamoune El Himri, Youness Achour and Hicham Yazid
Poly-disciplinary Faculty of Safi, Cadi Ayyad University, Laboratory of Analytical and Molecular Chemistry, Safi, Morocco

*Address all correspondence to: azizelkassimi2012@gmail.com

IntechOpen

© 2022 The Author(s). Licensee IntechOpen. This chapter is distributed under the terms of the Creative Commons Attribution License (<http://creativecommons.org/licenses/by/3.0>), which permits unrestricted use, distribution, and reproduction in any medium, provided the original work is properly cited. 

References

- [1] Anuar FI, Hadibarata T, Syafrudin M, Fona Z. Removal of Procion Red MX-5B from aqueous solution by adsorption on *Parkia speciosa* (stink bean) peel powder. *Biointerface Research in Applied Chemistry*. 2020;**10**:4774-4779
- [2] Katheresan V, Kansedo J, Lau SY. Efficiency of various recent wastewater dye removal methods: A review. *Journal of Environmental Chemical Engineering*. 2018;**6**:4676-4697
- [3] Slimani R, El Ouahabi I, Abidi F, El Haddad M, Regti A, Laamari MR, et al. Calcined eggshells as a new biosorbent to remove basic dye from aqueous solutions: thermodynamics, kinetics, isotherms and error analysis. *Journal of the Taiwan Institute of Chemical Engineers*. 2014;**45**(4):1578-1587
- [4] El Haddad M, Mamouni R, Saffaj N, Lazar S. Evaluation of performance of animal bone meal as a new low cost adsorbent for the removal of a cationic dye Rhodamine B from aqueous solutions. *Journal of Saudi Chemical Society*. 2016;**20**:S53-S59
- [5] Regti A, El Ayouchia HB, Laamari MR, Stiriba SE, Anane H, El Haddad M. Experimental and theoretical study using DFT method for the competitive adsorption of two cationic dyes from wastewaters. *Applied Surface Science*. 2016;**390**:311-319
- [6] Somsesta N, Sricharoenchaikul V, Aht-Ong D. Adsorption removal of methylene blue onto activated carbon/cellulose biocomposite films: Equilibrium and kinetic studies. *Materials Chemistry and Physics*. 2020;**240**:122221
- [7] Kristanti RA, Hadibarata T, Al Qahtani HMS. Adsorption of bisphenol A on oil palm biomass activated carbon: characterization, isotherm, kinetic and thermodynamic studies. *Biointerface Research in Applied Chemistry*. 2019;**9**:4217-4224
- [8] Sözüdoğru O, Fil BA, Boncukcuoğlu R, Aladağ E, Kul S. Adsorptive removal of cationic (BY2) dye from aqueous solutions onto Turkish clay: Isotherm, kinetic, and thermodynamic analysis. *Particulate Science and Technology*. 2016;**34**(1):103-111
- [9] Mukherjee K, Kedia A, Rao KJ, Dhir S, Paria S. Adsorption enhancement of methylene blue dye at kaolinite clay-water interface influenced by electrolyte solutions. *RSC Advances*. 2015;**5**:30654-30659
- [10] Turabik M. Adsorption of basic dyes from single and binary component systems onto bentonite: Simultaneous analysis of Basic Red 46 and Basic Yellow 28 by first order derivative spectrophotometric analysis method. *Journal of Hazardous Materials*. 2008;**158**(1):52-64
- [11] Lee YC, Kim JY, Shin HJ. Removal of malachite green (MG) from aqueous solutions by adsorption, precipitation and alkaline fading using talc. *Separation Science and Technology*. 2013;**48**:1093-1101
- [12] Tsai WT, Chang CY, Ing CH, Chang CF. Adsorption of acid dyes from aqueous solution on activated bleaching earth. *Journal of Colloid and Interface Science*. 2004;**275**:72-78
- [13] Gürses A, Karaca S, Doar C, Bayrak R, Açıkyıldız M, Yalçın M. Determination of adsorptive properties of clay/water system: methylene blue sorption. *Journal of Colloid and Interface Science*. 2004;**269**:310-314

- [14] Kausar A, Iqbal M, Javed A, Aftab K, Nazli ZH, Bhatti HN, et al. Dyes adsorption using clay and modified clay: A review. *Journal of Molecular Liquids*. 2018;**256**:395-407
- [15] Ferfera-Harrar H, Benhalima T, Sadi A. Development of functional chitosan-based superabsorbent hydrogel nanocomposites for adsorptive removal of Basic Red 46 textile dye. *Polymer Bulletin*. 2021:1-32
- [16] El Kassimi A, Achour Y, El Himri M, Laamari R, El Haddad M. Removal of two cationic dyes from aqueous solutions by adsorption onto local clay: Experimental and theoretical study using DFT method. *International Journal of Environmental Analytical Chemistry*. 2021:1-22
- [17] Nakarmi A, Bourdo SE, Ruhl L, Kanel S, Nadagouda M, Alla PK, et al. Benign zinc oxide betaine-modified biochar nanocomposites for phosphate removal from aqueous solutions. *Journal of Environmental Management*. 2020; **272**:111048
- [18] Dehmani Y, Lgaz H, Alrashdi AA, Lamhasni T, Abouarnadasse S, Chung IM. Phenol adsorption mechanism on the zinc oxide surface: Experimental, cluster DFT calculations, and molecular dynamics simulations. *Journal of Molecular Liquids*. 2021;**324**:114993
- [19] Yu S, Wang X, Ai Y, Tan X, Hayat T, Hu W, et al. Experimental and theoretical studies on competitive adsorption of aromatic compounds on reduced graphene oxides. *Journal of Materials Chemistry A*. 2016;**4**: 5654-5662
- [20] El Kassimi A, Boutouil A, El Himri M, Laamari R, El Haddad M. Selective and competitive removal of three basic dyes from single, binary and ternary systems in aqueous solutions: A combined experimental and theoretical study. *Journal of Saudi Chemical Society*. 2020;**24**(7):527-544
- [21] Regti A, El Ayouchia HB, Laamari MR, Stiriba SE, Anane H, El Haddad M. Experimental and theoretical study using DFT method for the competitive adsorption of two cationic dyes from wastewaters. *Applied Surface Science*. 2016;**390**:311-319
- [22] Achour Y, Khouili M, Abderrafia H, Melliani S, Laamari MR, El Haddad M. DFT investigations and experimental studies for competitive and adsorptive removal of two cationic dyes onto an eco-friendly material from aqueous media. *International Journal of Environmental Research*. 2018;**12**:789-802
- [23] Liu Y, Ma X, Li HA, Hou J. Competitive adsorption behavior of hydrocarbon (s)/CO₂ mixtures in a double-nanopore system using molecular simulations. *Fuel*. 2019;**252**: 612-621
- [24] Kohn W, Sham LJ. Self-consistent equations including exchange and correlation effects. *Physics Review*. 1965; **140**:A1133
- [25] Koopmans T. Ordering of wave functions and eigenenergies to the individual electrons of an atom. *Physica*. 1933;**1**:104-113
- [26] Schlegel HB. Geometry optimization on potential energy surfaces. In: *Modern Electronic Structure Theory: Part I*. 1995. pp. 459-500
- [27] Pearson RG. Hard and soft acids and bases. *Journal of the American Chemical Society*. 1963;**85**:3533-3539
- [28] Lesar A, Milošev I. Density functional study of the corrosion

inhibition properties of 1,2,4-triazole and its amino derivatives. *Chemical Physics Letters*. 2009;**483**:198-203

[29] Parr RG, Szentpaly LV, Liu S. Electrophilicity index. *Journal of the American Chemical Society*. 1999;**121**:1922-1924

[30] Domingo LR, Chamorro E, Pérez P. Understanding the reactivity of captodative ethylenes in polar cycloaddition reactions. A theoretical study. *The Journal of Organic Chemistry*. 2008;**73**:4615-4624

[31] Guo T, Wang K, Zhang G, Wu X. A novel α -Fe₂O₃@ g-C₃N₄ catalyst: Synthesis derived from Fe-based MOF and its superior photo-fenton performance. *Applied Surface Science*. 2019;**469**:331-339

[32] El Gaidoumi A, Benabdallah AC, Lahrichi A, Kherbeche A. Adsorption du phénol en milieu aqueux par une pyrophyllite marocaine brute et traitée (Adsorption of phenol in aqueous medium by a raw and treated moroccan pyrophyllite). *Journal of Materials and Environmental Science*. 2015;**6**:2247-2259

[33] Bellamy LJ. Amides, proteins and polypeptides. In: *The Infra-red Spectra of Complex Molecules*. Dordrecht: Springer; 1975. pp. 231-262

[34] Saikia BJ, Parthasarathy G, Borah RR, Borthakur R. Raman and FTIR spectroscopic evaluation of clay minerals and estimation of metal contaminations in natural deposition of surface sediments from Brahmaputra river. *International Journal of Geosciences*. 2016;**7**:873-883

[35] Miyah Y, Lahrichi A, Idrissi M, Anis K, Kachkoul R, Idrissi N, et al. Removal of cationic dye "crystal violet" in

aqueous solution by the local clay. *JMES*. 2017;**8**(10):3570-3582

[36] Aroke UO, Abdulkarim A, Ogubunka RO. Fourier-transform infrared characterization of kaolin, granite, bentonite and barite. *ATBU Journal of Environmental Technology*. 2013;**6**:42-53

[37] Kousha M, Daneshvar E, Salar-Sohrabi M, Jokar M, Bhatnagar A. Adsorption of acid orange II dye by raw and chemically modified brown macroalga *Stoechospermum marginatum*. *Chemical Engineering Journal*. 2012;**192**:67-76

[38] Singh H, Choden S. Comparison of adsorption behaviour and kinetic modeling of bio-waste materials using basic dye as adsorbate. *Indian Journal of Chemical Technology*. 2015;**21**:359-367

[39] Ghasemian Lemraski E, Sharafinia S, Alimohammadi M. New activated carbon from Persian mesquite grain as an excellent adsorbent. *Physical Chemistry Research*. 2017;**5**:81-98

[40] Zhang L, Hu P, Wang J, Huang R. Crosslinked quaternized chitosan/bentonite composite for the removal of Amino black 10B from aqueous solutions. *International Journal of Biological Macromolecules*. 2016;**93**:217-225

[41] Kausar A, Shahzad R, Iqbal J, Muhammad N, Ibrahim SM, Iqbal M. Development of new organic-inorganic, hybrid bionanocomposite from cellulose and clay for enhanced removal of Drimarine Yellow HF-3GL dye. *International Journal of Biological Macromolecules*. 2020;**149**:1059-1071

[42] Ngwabebhoh FA, Erdem A, Yildiz U. Synergistic removal of Cu (II) and nitrazine yellow dye using an eco-friendly chitosan-montmorillonite

hydrogel: Optimization by response surface methodology. *Journal of Applied Polymer Science*. 2016;**133**(29)

[43] Wang Y, Wang W, Wang A. Efficient adsorption of methylene blue on an alginate-based nanocomposite hydrogel enhanced by organo-illite/smectite clay. *Chemical Engineering Journal*. 2013;**228**:132-139

[44] El Mouzdahir Y, Elmchaouri A, Mahboub R, Gil A, Korili SA. Equilibrium modeling for the adsorption of methylene blue from aqueous solutions on activated clay minerals. *Desalination*. 2010;**250**:335-338

[45] Rahmat M, Rehman A, Rahmat S, Bhatti HN, Iqbal M, Khan WS, et al. Highly efficient removal of crystal violet dye from water by MnO₂ based nanofibrous mesh/photocatalytic process. *Journal of Materials Research and Technology*. 2019;**8**(6):5149-5159

[46] Auta M, Hameed B. Chitosan–clay composite as highly effective and low-cost adsorbent for batch and fixed-bed adsorption of methylene blue. *Chemical Engineering Journal*. 2014;**237**:352-361

[47] Gao W, Zhao S, Wu H, Deligeer W, Asuha S. Direct acid activation of kaolinite and its effects on the adsorption of methylene blue. *Applied Clay Science*. 2016;**126**:98-106

[48] Gao Z, Li X, Wu H, Zhao S, Deligeer W, Asuha S. Magnetic modification of acid-activated kaolin: Synthesis, characterization, and adsorptive properties. *Microporous and Mesoporous Materials*. 2015;**100**(202):1-7

[49] Kausar A, Iqbal M, Javed A, Aftab K, Bhatti HN, Nouren S. Dyes adsorption using clay and modified clay: A review. *Journal of Molecular Liquids*. 2018;**256**:395-407

[50] Şahin Ö, Kaya M, Saka C. Plasma-surface modification on bentonite clay to improve the performance of adsorption of methylene blue. *Applied Clay Science*. 2015;**116**:46-53

[51] Ai L, Zhou Y, Jiang J. Removal of methylene blue from aqueous solution by montmorillonite/CoFe₂O₄ composite with magnetic separation performance. *Desalination*. 2011;**266**:72-77

[52] Bolster CH, Hornberger GM. On the use of linearized Langmuir equations. *Soil Science Society of America Journal*. 2007;**71**(6):1796-1806

[53] Şişmanoğlu T. Corrigendum to “Removal of some fungicides from aqueous solution by the biopolymer chitin” [*Colloid Surf. A: Physicochem. Eng. Aspects* 297 (2007) 38–45]. *Colloids and Surfaces A: Physicochemical and Engineering Aspects*. 2007;**3**:257

[54] Freundlich HMF. Over the adsorption in solution. *The Journal of Physical Chemistry*. 1906;**57**(385471):1100-1107

[55] Ergene A, Ada K, Tan S, Katırcıoğlu H. Removal of Remazol Brilliant Blue R dye from aqueous solutions by adsorption onto immobilized *Scenedesmus quadricauda*: Equilibrium and kinetic modeling studies. *Desalination*. 2009;**249**:1308-1314

[56] Aziz EK, Abdelmajid R, Rachid LM, Mohammadine EH. Adsorptive removal of anionic dye from aqueous solutions using powdered and calcined vegetables wastes as low-cost adsorbent. *Arab Journal of Basic and Applied Sciences*. 2018;**25**(3):93-102

[57] Ho YS, McKay G. Sorption of dye from aqueous solution by peat. *Chemical Engineering Journal*. 1998;**70**(2):115-124

[58] Weber WJ, Morris JC, Sanit J. Kinetics of adsorption on carbon from solution. *Journal of the Sanitary Engineering Division*. 1963;**89**(2):31-59

[59] Varjani S, Rakholiya P, Ng HY, You S, Teixeira JA. Microbial degradation of dyes: an overview. *Bioresource Technology*. 2020;**314**:123728

[60] Almeida CAP, Debacher NA, Downs AJ, Cottet L, Mello CAD. Removal of methylene blue from colored effluents by adsorption on montmorillonite clay. *Journal of Colloid and Interface Science*. 2009;**332**(1):46-53

[61] Chamorro E, Pérez P, Domingo LR. On the nature of Parr functions to predict the most reactive sites along organic polar reactions. *Chemical Physics Letters*. 2013;**582**:141-143

[62] Sintakindi A, Ankamwar B. Fungal biosorption as an alternative for the treatment of dyes in waste waters: A review. *Environmental Technology Reviews*. 2021;**10**(1):26-43